J. Nanoanalysis., 6(4): 217-227, Autumn 2019

ORIGINAL RESEARCH PAPER

Synthesis of Fe_3O_4/Eggshell and egg membrane Nanocomposite and Application for Adsorption of Cationic and Anionic Dyes

Naereh Besharati, Nina Alizadeh*

Department of Chemistry, University of Guilan, Rasht, Iran

Received: 2018-07-01 Accepted: 2019-07-15 Published: 2019-09-20

ABSTRACT

This work is reported on the synthesis of Fe_3O_4/eggshell nanocomposites in the absence of any stabilizer or surfactant. Fe_3O_4 magnetic nanoparticles were established on the egg shell. The adsorption of Malachite green (MG) and Crystal violet (CV) as cationic dyes and Eriochrome Black T (EBT) as an anionic dye by magnetite nanoparticles loaded egg shell (MNLES) and magnetite nanoparticles loaded egg membrane (MNLEM) were studied. FT-IR, XRD and SEM were used for specification of adsorbents. XRD pattern of MNLES and MNLEM were corresponded to pure magnetite at 2θ= 30.2°, 35.6°, 43.3° and 57.2°. FTIR showed that main peak similar magnetite in 580, 1620 and 3407cm^{-1}. SEM pictures showed that Fe_3O_4 nanoparticles in nm size loaded on natural adsorbents. Adsorbents dose, pH and contact time as parameters that have an effect on dye removal were investigated. Pseudo-first order, pseudo-second order, intraparticle diffusion and Elovich models were used for study of kinetic of adsorption. The sorption of the MG, EBT, CV on the MNLEM were pseudo second-order model. The sorption of the MG and EBT on MNLES were described by Elovich and pseudo second-order model. Value of q_{max} from the Langmuir model for adsorption of CV, EBT and MG were 61.72, 21.69 and 38.31mg g^{-1} for MNLEM and q_{max} for adsorption of EBT, MG on the MNLES was 40.0 and 25.12mg g^{-1}. It was found MNLES and MNLEM can be used as efficient adsorbents for removal of EBT more than cationic dyes (MG, CV).

Keywords: *Malachite green, Crystal violet, Eriochrome Black T, Egg shell and Egg membrane, Magnetic nanoparticles*

How to cite this article

*Besharati N, Alizadeh N. Synthesis of Fe_3O_4/Eggshell and egg membrane Nanocomposite and Application for Adsorption of Cationic and Anionic Dyes. J. Nanoanalysis., 2019; 6(4): 217-227. DOI: 10.22034/jna.****

INTRODUCTION

Application of bio-waste materials such as eggshell waste is the strategy of using waste materials. Low-cost eggshell waste has been widely used as a possible bone substitute, catalyst, support, and efficient bio-templates due to their high catalytic activity, ease of handling and reusability. The eggshell is an inexpensive and easily available biomaterial; it has porous structure that is related to its natural content [1-7]. Egg shells are one of the widely used food processing and manufacturing plant by-products. Eggs represent a major ingredient in a large variety of products in restaurants, whose production results in several daily tons of eggshell waste and incur considerable disposal costs in the world. About 250000 tons of eggshell waste are produced annually worldwide. Nowadays eggshell as green and economical adsorbents use for removing hydrogen sulphide and heavy metals from wastewater, so in this research MNLES and MNLEM were used for removing cationic and anionic dye. Eggshell can be widely used as a good adsorbent because of ease of handling, reusability and its low-cost waste. Many industries use dyes and pigments for coloring purposes [8]. Toxic, carcinogenic effects on humans and aesthetic effect on the aquatic environment arises from dye contamination [9]. Dyes remain in the natural

* Corresponding Author Email: *n–alizadeh@guilan.ac.ir*

environment due to the persistence and non-degradation of their aromatic structure. Malachite green (MG) is a synthetic, and an organic compound that is used as a dye in silk, wool, jute, leather, cotton, fabric, papers and acrylic industries [10]. If it is used as a parasiticide and antibacterial chemical in fish, its residues cause carcinogenesis, mutagenesis, chromosomal fractures [11-13]. Crystal violet (CV) is a synthetic cationic dye from the triarylmethane group [14] and CV is used in black inks and for dyeing purposes such as silk, nylon, wool. It is toxic and in high value it causes eye discomfort, kidney diseases and cancer so there are interests for eliminate CV from water environment. Medically, CV is used for the treatment of burns, boils and mycotic skin infections and it has an antiseptic effect on gram-positive organisms [16]. Eriochrome black-T (EBT) is used for biological coloring, dyeing silk, wool, nylon multifibers. Determination of Ca^{2+}, Mg^{2+} and Zn^{2+} is done with complexometric method by using EBT. Dye is hazardous and its degradation product is still carcinogenic [17]. Adsorption between different methods for dye removal because of low cost, to be effective and usability is the acceptable method [18, 19]. Nowadays nanotechnology develops and is used for wastewater treatment because it is affordable, trustworthy, fast and lasting [20]. Different agricultural waste materials such as palm shell [21], grapefruit peel [22], pine cone [23], pine tree leaves [24], pomelo skin based AC [25], banana pith [26], bio waste material [27], powdered waste sludge [28], wheat shells [29], palm shell powder, chitozan [30] and Coffee waste [31] are used for pollution elimination. Recent research has proven that magnetic nanoparticles, due to their unique properties act as a suitable adsorbent to remove pollutants. Intended compound and pollutants can be separate from a solution with magnetic separation [32-37]. Co-precipitation is an easy method for production of Iron oxide, magnetite nanoparticles (MNPs) [38-40]. So, this study focused on egg shell and egg membrane modified with magnetite nanoparticles as adsorbents for removal of MG, CV and EBT dyes and pseudo-first order, pseudo-second order, Elovich and intra-particle diffusion for kinetic models were examined. Finally, optimum conditions, Isotherm models as Langmuir, Freundlich and temkin were evaluated to obtain highest dye removal capacity.

MATERIAL AND METHODS

General

Malachite green (MG) and crystal violet (CV) as cationic dyes and eriochrome black T (EBT) as an anionic dye as shown in Fig. 1(a,b,c), Ferric chloride hexahydrate ($FeCl_3.6H_2O$), ferroussulphate heptahydrate ($FeSO_4.7H_2O$), amonia, hydrochloric acid and sodium hydroxide with the highest purity were obtained from Merck (Germany). Stock and working solutions of dyes ($C_{CV, MG}$= 4 mg L^{-1}, C_{EBT} = 40 mg L^{-1}) were prepared in double distilled water show the molecular structure of CV, MG and EBT. Dye removal were done with calibration curve and improving of effective factors.

Dye adsorbtion measurements were done at λ_{max}= 596, 620 and 530 nm, for CV, MG and EBT, respectively that, were chosen as maximum absorbance wavelength from calibration curve

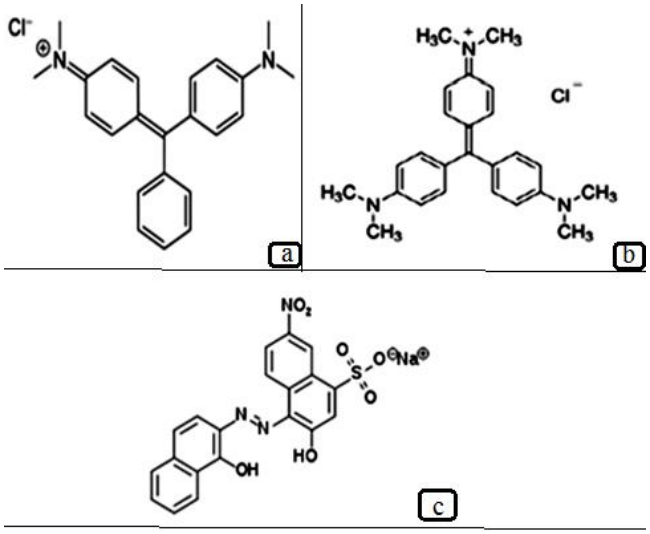

Fig. 1. Chemical structure of MG (a), CV (b), EBT (c).

with a spectrophotometer Jenway (model 6105, England). pH measurements were done with A Jenway pHmeter (model 370, England). The infrared spectra of Egg shell, Egg membrane, MNLES and MNLEM were studied in the range of 500-3500 cm^{-1} by an infrared instrument (FT-IR, model Alfa, Germany). Morphology of prepared samples was obtained by a SEM device (model EM3200, USA). X-ray diffraction (XRD) measurement were done with philips diffractometer with mono chromatize Cu radiation (model Xpert MPD, Holland) . Egg shell and Egg membrane were crushed with Grinder (model MCG 1575, China) and stirring of solutions were done with rotator (IKA, MS3 basic). Strong magnet 1.4 T was used for separation based on magnetic properties.

Preparation of the adsorbents

Egg shell and egg membrane collected, washed and dried in oven at 105°C of, they were crushed and sieved to 150-200 µm particle size. Then the powder was dried at 105°C for 24 hours to remove moisture and stored in a closed bottle for later use in adsorption studies.

Preparation of magnetic nanoparticles loaded Egg shell and Egg membrane

Magnetite nanoparticle loaded Egg shell (MNLES) and magnetite nanoparticle loaded Egg membrane (MNLEM) were prepared by coprecipitation method. Fe^{2+}/Fe^{3+} solution were prepared by dissolving $FeCl_3.6H_2O$ (6.1 g) and $FeSO_4.7H_2O$ (4.2 g) in 100 mL distilled water and heating to 90°C. Then 200 mL of distilled water, which contains 10 mL of ammonium hydroxide (28% w/w) and 1 g of Egg shell powder and egg membrane powder (separately for prepration of MNLES and MNLEM) were added rapidly to this solution. The mixture was mixed at 80°C for 30 min while pH was regulated in 10 and then cooled to room temperature. Then Fe_3O_4–egg shell (MNLES) and Fe_3O_4–egg membrane (MNLEM) were stored after filtering, washing with distilled water, drying at 50°C (24 h). MNLES and MNLEM adsorbents were attracted by the magnet as shown in Fig. 2 (c, f). Magnetic properties of the synthesized nanoparticles are clearly observed.

EDX revealed that MNLES and MNLEM have 34.57% and 20.75% Fe and 1 g egg shell and Egg

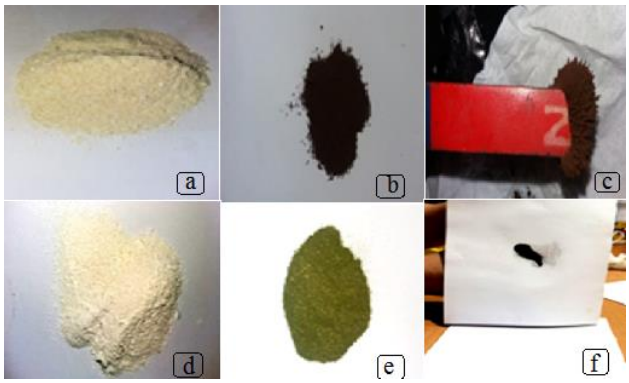

Fig. 2. (a) Pretreated Egg shell, (b) MNLES, and (c) MNLES totally attracted to magnet, (d) pretreated Egg membrane, (e) MNLEM, and (f) MNLEM totally attracted to magnet.

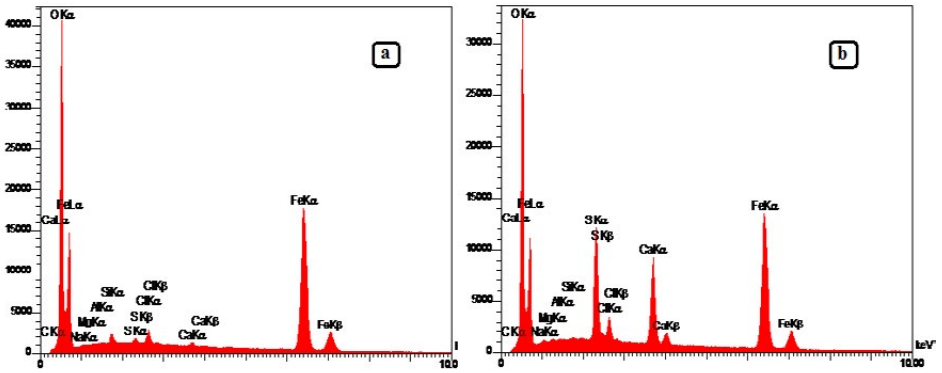

Fig. 3. EDX of (a) MNLES and (b) MNLEM

membrane have 0.47 and 0.28 g Fe_3O_4 respectively (Fig. 3).

RESULTS AND DISCUSSION

Synthesis and characterization

XRD and SEM instruments were used to emphasis on creating properties of the synthesized MNLES and MNLEM. Fig. 4 shows the SEM images of MNLES and MNLEM and pretreated Egg shell, Egg membrane. Magnetite nanoparticles as shown in images, sitting on surface of egg shell and egg membrane.

The XRD pattern of MNLES and MNLEM in Fig. 5. show typical patterns of magnetite at 2θ= 30.2°, 35.6°, 43.3° and 57.2° which are corresponded with pure magnetite. The results confirm that

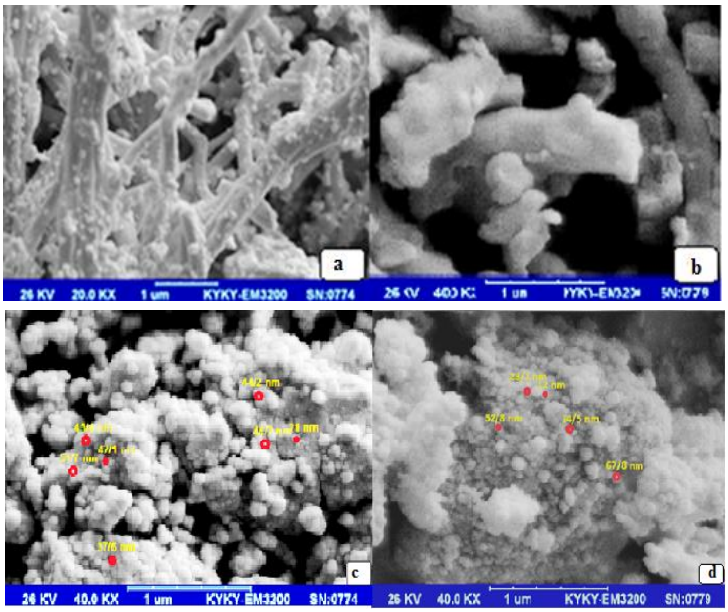

Fig. 4. The SEM image of (a) pretreated egg shell, (b) MNLES, (c) pretreated egg membrane and (d) MNLEM.

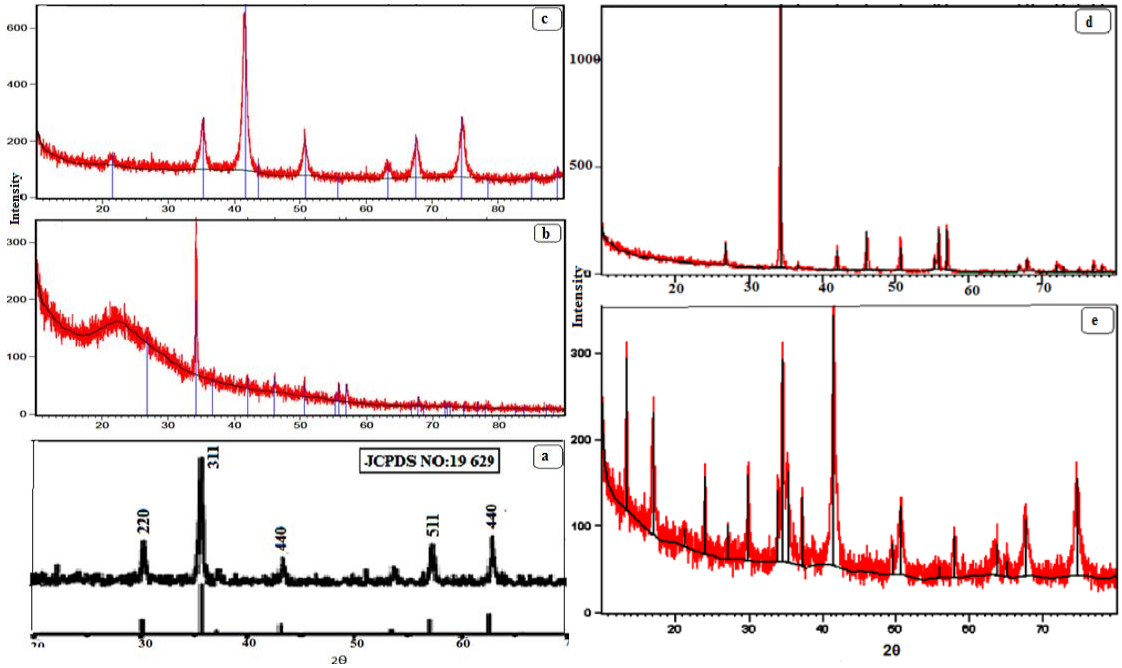

Fig. 5. XRD pattern of (a) Magnetite, (b) pretreated egg membrane(c) MNLEM, (d)pretreated egg shell and (e) MNLES

the surfaces of egg shell and egg membrane are successfully covered with Fe_3O_4 nanoparticles. The average crystallite size of NPs by the Scherer equation according to the XRD pattern for MNLES was 11.5 nm and for MNLEM was 12 nm.

The FT-IR spectra of egg shell and egg membrane after and before modifying and spectra of Fe_3o_4 magnetite shown in Fig. 6. The spectra display absorption bands related to magnetite nanoparticles and also different bands about Egg shell and Egg membrane.

FT-IR analysis showed –OH groups with a band at 3420 cm^{-1}. Aliphatic C–H groups confirmed with the band at 2850–2920 cm^{-1}. The strong band at 1638–1648 cm^{-1} represents the C=C stretching vibrations. The absorbtion band around 1380-1415cm^{-1}, represents S=O is stretching of sulfate. The band observed at about 710 and 870cm^{-1} could be assigned to the alkene C=C bond. The FT-IR spectrum of MNLES and MNLA show strong band in the low-frequency region (500–1000 cm^{-1}) due to iron oxide skeleton, which is in agreement with the magnetite spectrum. The peak at 1150 cm^{-1} showed the stretching bond of Fe–O and the peak at 1633 cm^{-1} and 3446 cm^{-1} implied the existence of residual hydroxyl groups. The intensity of these bonds in MNLES and MNLEM is higher than egg shell and egg membrane. It observed that there were main peaks in magnetite were in MNLES and MNLEM. Thus, all the above results indicate that the magnetic nanoparticles were loaded on the Egg shell and Egg membrane.

Dye adsorption optimization

Different parameters affecting the removal of dyes were studied to prepare maximum adsorption.

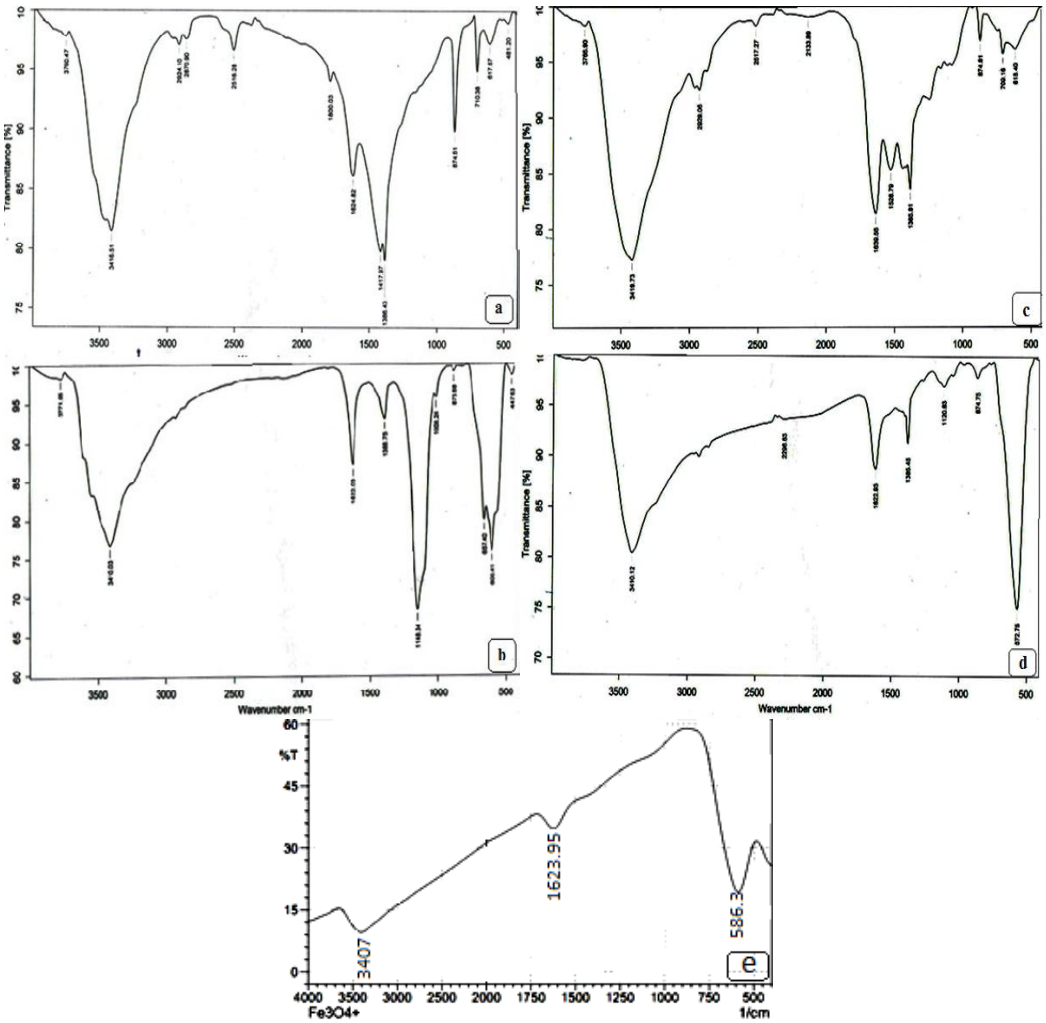

Fig. 6. FT-IR spectra of (a) pretreated egg shell, (b) MNLES, (c) pretreated egg membrane and (d) MNLEM and(e) magnetite Fe_3O_4.

Effect of different pHs on absorption of dyes was investigated with measuring absorbance of CV and MG solutions (4 mg L^{-1}) at 596 and 620 nm, as well as EBT solution (40 mg L^{-1}) at 530 nm. For optimization studies, suitable amount of adsorbent (MNLES or MNLEM) were added to 20mL solution of each dye at various concentrations in a 50 mL beaker and pH of the solution with HCl and NaOH (0.1 mol L^{-1}), was regulated to the intended amount. After adsorption of dyes during the proper time for mixing, spectrophotometer was used for determining residual dye concentrations by using calibration curve after separation of adsorbents with strong magnet. This equation was used to calculate the dye removal in the experiments:

$$\%R= \frac{C_0 - C_t}{C_0} \times 100 \quad (1)$$

C_o and C_t are the first and remaining concentrations of the dyes after removal by synthesized adsorbents.

Effect of adsorbent amount on the dyes removal efficiency

Adsorbents amount in the range of 0.01–0.07 g (0.5-3.5 g L^{-1}) at optimum pH in contact with 20 mL solution of 4mg L^{-1} of CV and MG and 40 mg L^{-1} of EBT were used for research on the effect of adsorbent amount for dyes removal. Collision rate of dyes with adsorbents and also more accessiblity of adsorbents increase as a result of increasing the amount of adsorbents, So removal efficiency increase. The removal efficiency of MG reached maximum with 0.03 g (1.5 g L^{-1}) of MNLES and MNLEM and for EBT reached maximum with 0.05g (2.5 g L^{-1}) and 0.03g (1.5 g L^{-1}) of MNLES and MNLEM, respectively. Also, the removal efficiency of CV was achieved maxium using 0.05 g (2.5 g L^{-1}) of MNLEM. But, MNLES dosen't have high removal efficiency for CV (Fig. 7).

Effect of contact time on the MG, CV, EBT removal efficiency

Adsorption of dyes for review of the contact time effect on the adsorption of CV and MB (4 mg L^{-1}) and EBT (40 mg L^{-1}) from solution were studied. Different times were used to measure absorbance of the residual solution. It was observed that 55.3 % of MG was adsorbed with MNLES after 35 min and this time is suitable for maximum removal of dye. Removal efficiency was reached to 58.7 % after 40 min. Also, MNLEM showed maximum adsorption for MG from 35 to 40 min (48.9 % to 51.9 %) (Fig. 7). Therefore 35 min was selected as a suitable time for further works. MNLEM had 53.8 to 61.6 elimination percent for CV with varying time from 40 to 60 min. Also, MNLES showed low removal efficiency as 16.4 % after 40 min and had not good adsorption for CV (Fig. 8). For EBT, the elimination percent varied from 79.5 to 81.3 % using MNLES and during changing time from 20 to 40 min. Also, MNLEM showed 69.0 to 77.0 %removal during changing contact time from 10 to 20 min (Fig. 8).

Effect of pH on the MG, CVand EBT elimination percent

Effect of pH on removal of dyes investigated in the range of 3.0–12.0 at a suitable time for mixing of solution. Fig. 9 shows the removal efficiency of dyes as a function of pH. At lower pH, surface of adsorbent has a positive charge and in higher pH, surface of adsorbent has negative cherge, so anionic and cationic cantamination absorbed on

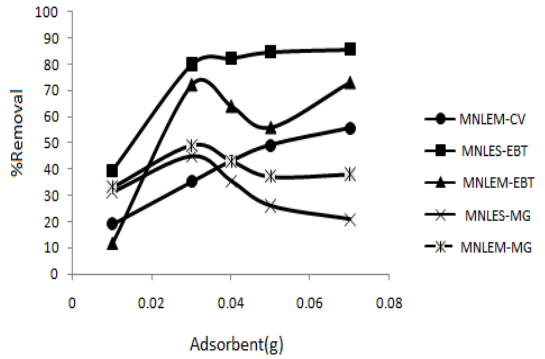

Fig. 7. Effect of amount of adsorbents on the removal efficiency of CV, MG and EBT ($C_{CV, MG}$ =4 mg L^{-1}, C_{EBT} = 40 mg L^{-1} , V = 20 mL).

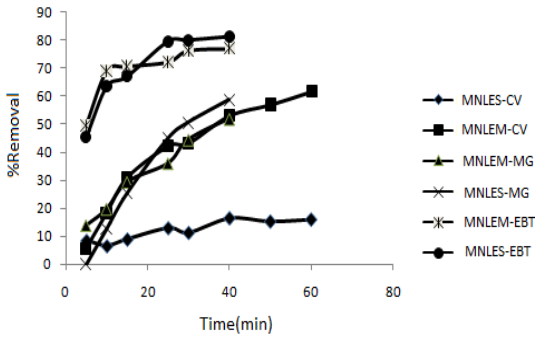

Fig. 8. Effect of contact time on the removal efficiency of CV, MG and EBT ($C_{CV, MG}$ =4 mg L^{-1}, C_{EBT} = 40 mg L^{-1} , V = 20 mL).

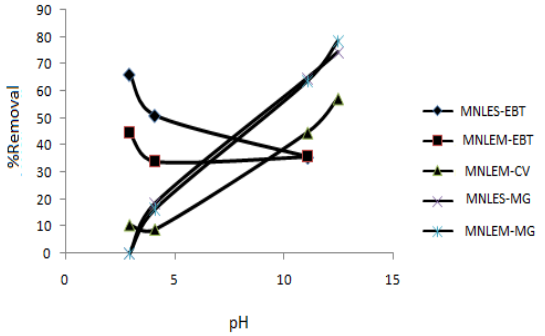

Fig. 9. Effect of pH of solution on the CV, MG and EBT removal ($C_{CV, MG}$=4 mg L^{-1}, C_{EBT} = 40 mg L^{-1} , V = 20 mL).

it respectively. This is related to the effect of pH chemistry of solution and acceptance-sites of surface. The adsorption increased by increasing solution pH and reached maximum at pH=7-12 for cationic dyes (MG and CV). For EBT as an anionic dye, the removal efficiency was increased by decreasing solution pH and reached maximum at pH=3-7.

The study of kinetic and adsorption isotherms

The study of kinetics of CV, EBT and MG adsorption onto MNLES and MNLEM adsorbents are required for selecting optimum operating conditions for the full-scale removal processes. The kinetic parameters, which are helpful for the prediction of the adsorption rate, give important information for designing and modeling of the adsorption processes [40-43]. The kinetic data for adsorption onto MNLES and MNLEM were analyzed using pseudo-first order, pseudo-second order, Elovich and intra-particle diffusion models to find out the adsorption rate expressions. The correlation between experimental data and the kinetic models are expressed by the correlation coefficients (R^2, values close to 1) and show the influence of time on the dye removal efficiency. In the present study, kinetic studies were performed in the time intervals ranged from 0 to 30 min. After contact between the adsorbents and solution of each dye (separately) during the time intervals, the clear supernatant solutions were spectrophotometrically measured for residual CV, EBT and MG concentration in the solution. Fig. (10, 11) show the equilibrium concentrations of CV and MG at the adsorption time interval of 0–30min. The concentration of residual CV, EBT and MG in the solution was monitored and the adsorption capacity at time t (q_t, mg g^{-1}) was calculated by the following equation:

$$q_t = \frac{(C_0 - C_t) \times V}{W} \quad (2)$$

Where C_o and C_t are the initial and equilibrium concentrations (mg L^{-1}) of dyes at a given time t, respectively. Also, V is the solution volume (mL) and W is the weight of the adsorbent (g). The removal rate was very fast during the initial stages of the adsorption processes. The kinetic of adsorption was obtained as a pseudo-second order according to the following equation. The pseudo-second order reaction rate may be dependent on the amount of solute adsorbed on the surface of adsorbent and the amount adsorbed at equilibrium. The kinetic rate equations for pseudo-second order reaction can be written as follows:

$$\frac{t}{q_t} = \frac{1}{K_2 q_e^2} + \left[\frac{1}{q_e}\right] t \quad (3)$$

Where q_t and q_e, are the value of adsorbed dye at each time and at equilibrium and k_2 (g mg^{-1} min^{-1}

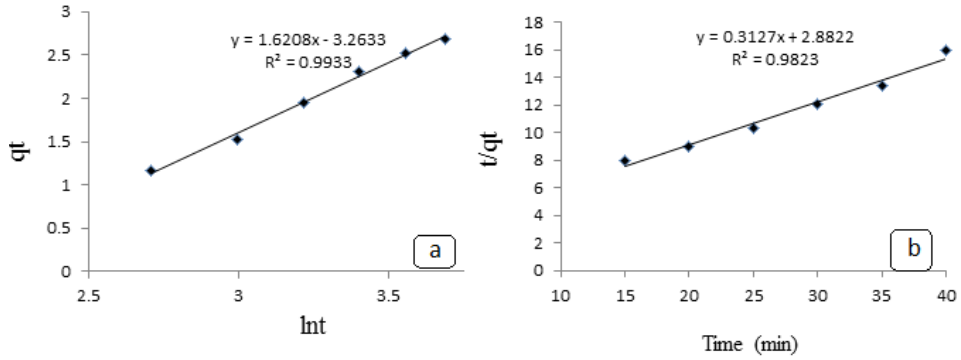

Fig. 10. Fitting of kinetic data of the MG removal to the Elovich and pseudo-second order kinetic models for MNLES and MNLEM adsorbents, respectively (pH=9, adsorbent mass: 0.03 g (1.5 g L^{-1}), C_{MG} =3 mg L^{-1} for (a) MNLESand (b)MNLEM).

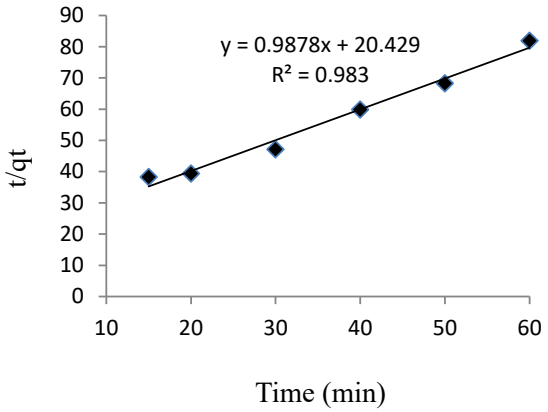

Fig. 11. Fitting of kinetic data of the CV to the pseudo-second order kinetic model for MNLEM (pH=9, MNLEM=0.03 g(1.5 g L^{-1}), C_{CV} =3 mg L^{-1}).

^{1}) is the pseudo-second order rate constant. If the second order kinetic equation is applicable, the plot of t/q_t against t (Eq.(3)) should give a linear relationship. The q_e and k_2 can be determined from the slope and intercept of the plot. Fitting of kinetic data to pseudo-second order kinetic model, was shown in Figs. 10-12. The best fit of the pseudo-second order kinetic model (R^2 close to 1) in the present system shows the adsorption of MG, CV and EBT for MNLEM and EBT for MNLES followed of chemisorptions mechanism via electrostatic attraction.

Equilibrium isotherm equations are used to describe the experimental sorption data. The parameters obtained from the different models provide important information on the sorption mechanisms and the surface properties and affinities of the sorbent. The equilibrium adsorption isotherm was determined using batch studies(Table 1). 20 mL of the dye solution with various initial dye concentrations was poured into a glass bottle. The time required to reach equilibrium as determined in equilibrium studies was 30 min. The amount of dye uptake by the MNLES and MNLEM, q_e (mg g^{-1}), was obtained by equation (2).

Adsorption data obtained in a concentration range of 10–50 mg L^{-1} were correlated with the following linear forms of Langmuir (Eq. (4)) [44] and Freundlich (Eq. (5)))) [45] and Tempkin (Eq. (6)) [46].

adsorption isotherm models:

Langmuir equation:

$$\frac{C_e}{q_e}=\frac{1}{K_l q_{max}}+\frac{1}{q_{max}}c_e \qquad (4)$$

Freundlich equation:

$$\log q_e=\log K_f+\frac{1}{n}\log c_e \qquad (5)$$

Tempkin equatin:

$$q_e=K_1.\ln(K_2)+K_1.\ln(c_e) \qquad (6)$$

Where q_e is the equilibrium dye concentration on the adsorbent (mg g^{-1}), C_e is the equilibrium dyes concentration in the solution (mg L^{-1}), q_{max} is the monolayer capacity of the adsorbent (mg g^{-1}), K_L is the Langmuir constant (L mg^{-1}) and is related to the free energy of adsorption, K_F is the Freundlich constant (L g^{-1}) and n (dimensionless) is the heterogeneity factor.

In the Langmuir model, a plot of Ce/qe versus Ce should indicate a straight line of slope $1/q_{max}$ and an intercept of $1/(K_L q_{max})$. K_1 is related to the heat of adsorption (L g^{-1}) and K_2 is the dimensionless Tempkin isotherm.

The correlation coefficient for the adsorption isotherm study of CV ($R^2_{Langmuir}$=0.9642, $R^2_{Freundlich}$= 0.9633), EBT ($R^2_{Langmuir}$=0.9912, $R^2_{Freundlich}$=0.6727) and MG ($R^2_{Langmuir}$=0.9678, $R^2_{Freundlich}$= 0.957)

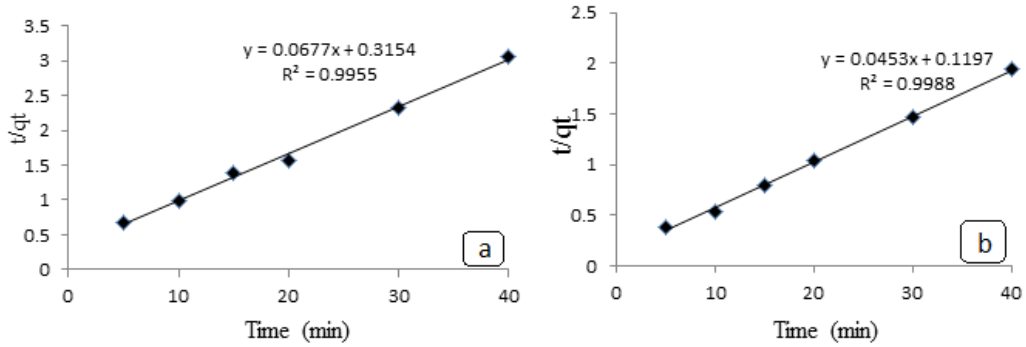

Fig. 12. Fitting of kinetic data of the EBT to the pseudo-second order kinetic model (pH=4, MNLES= 0.05 g (2.5 g L^{-1}), MNLEM= 0.03 g(1.5 g L^{-1}), C_{EBT} =40 mg L^{-1} for (a) MNLES and (b) MNLEM).

Table 1. The values of parameters obtained by different kinetic models

Kinetic models	Parameters	MNLES dye		MNLEM dye		
		EBT	MG	CV	MG	EBT
Pseudo-first order	K_1 (min^{-1})	1.46	0.014	0.0217	0.023	0.02
	$q_{e,cal}$ ($mg\ g^{-1}$)	4.32	1.103	0.056	0.227	1.858
	R_1^2	0.7219	0.0403	0.3912	0.058	0.1323
Pseudo-second order	k_2 ($g\ mg^{-1}\ min^{-1}$)	0.014	4.25×10^{-4}	0.047	0.033	0.017
	$q_{e,cal}$ ($mg\ g^{-1}$)	14.77	14.224	1.012	3.19	22.07
	R_2^2	0.9955	0.6551	0.983	0.982	0.9988
Elovich	ß	0.35	0.616	4.06	25.83	0.306
	α	8.88	12.11	0.091	1.7×10^{23}	58.82
	R^2	0.921	0.9933	0.9547	0.979	0.8493

Table 2. The constants values of different adsorption models.

Isotherm models	Parameters	Adsorbent MNLES Dye			MNLEM Dye	
		EBT	MG	CV	MG	EBT
Langmuir	q_{max} ($mg\ g^{-1}$)	40	25.12	61.72	38.31	21.69
	R^2	0.9889	0.8908	0.9642	0.9678	0.9912
	K_1 ($L\ mg^{-1}$)	0.04	0.12	-0.736	-0.42	7.81
Freundlich	K_F	2.07	156.31	600.48	1.9×10^{3}	18.31
	n	1.34	1.35	-3.61	-0.54	14.53
	R^2	0.9909	0.9809	0.9633	0.957	0.6727
Temkin	K_1	6.9061	1819	-0.27	-373.03	1.234
	R^2	0.9683	0.7402	0.806	0.7623	0.6502
	K_2	0.67	1.024	0.139	0.138	3.72×10^{6}

(Table 2) on the MNLEM adsorbent showed strong positive evidence that the adsorption of dyes follows the Langmuir isotherm. This indicates that the adsorption of dyes occurs on a homogenous surface by monolayer adsorption without any interaction between adsorbed ions. The obtained value of q_{max} from the Langmuir model for adsorption of CV, EBT and MG were 61.72, 21.69 and 38.31mg g^{-1} for MNLEM respectively.

The correlation coefficient for EBT ($R^2_{Langmuir}$=0.9889, $R^2_{Freundlich}$= 0.9909) and MG ($R^2_{Langmuir}$=0.8908, $R^2_{Freundlich}$= 0.9809) for MNLES showed that adsorption of dye onto adsorbents follows the Freundlich isotherm more than Langmuir model. The value of q_{max} for adsorption of EBT and MG on the MNLES was 40.0 and 25.12mg g^{-1}, respectively.

CONCLUSION

The sorption of pollutants from aqueous solutions plays a significant role in water pollution control. The MNLES and MNLEM are synthesized easily. Due to their very high surface areas, high adsorption capacity can be achieved using magnetic nanoparticles loaded them. For this purpose, the utilization of the MNLES and MNLEM as efficient adsorbents were successfully carried out for removal of MG, EBT, CV. XRD pattern of MNLES and MNLEM were corresponded to pure magnetite at 2θ= 30.2°, 35.6°, 43.3° and 57.2°. FTIR showed that main peak in 580, 1620 and 3407cm^{-1} in MNLES and MNLEM similar magnetite. SEM pictures showed that nanoparticles loaded with natural adsorbents in nm size. XRD pattern of MNLES and MNLEM were corresponded to pure magnetite at 2θ= 30.2°, 35.6°, 43.3° and 57.2°. EDX revealed that MNLES and MNLEM have 34.57% and 20.75% Fe and 1 g Egg shell and Egg membrane have 0.47 and 0.28 g Fe_3O_4 respectively. The results confirm that the surfaces of egg shell and egg membrane are successfully covered with Fe_3O_4 nanoparticles. The adsorption followed the pseudo-second order kinetic model, suggesting chemisorption mechanism. The fit of the Langmuir

model on the adsorption data of MNLEM for CV($R^2_{Langmuir}$=0.9642), EBT($R^2_{Langmuir}$=0.9912) and MG ($R^2_{Langmuir}$=0.9678) in the present system shows the formation of a monolayer covering of the adsorbate at the outer space of the adsorbent. The obtained value of q_{max} from the Langmuir model for adsorption of CV, EBT and MG were 61.72, 21.69 and 38.31mg g^{-1} for MNLEM respectively. For MNLES adsorption data of MG and MG ($R^2_{Freundlich}$= 0.9809)and EBT($R^2_{Freundlich}$= 0.9909) were fitted well to the Freundlich model. The value of q_{max} for adsorption of EBT and MG on the MNLES was 40.0 and 25.12mg g^{-1}, respectively. The data reported here should be useful for the design and fabrication of an economical treatment process for dye adsorption in industrial effluents.

ACKNOWLEDGMENT

Authors acknowledge financial support from Reseach Consil of University of Guilan.

CONFLICT OF INTEREST

The authors declare that there is no conflict of interests regarding the publication of this manuscript.

Symbols

MNLES: Magnetite nanoparticles loaded green egg shell.
MNLEM: Magnetite nanoparticles loaded egg membrane.
q_e: equilibrium dye concentration on the adsorbent.
C_e: equilibrium dye concentration in the solution.
q_{max}: monolayer capacity of the adsorbent.
K_L: Langmuir constant.
K_F: Freundlich constant.
N: Degree of nonlinearity of adsorption.

REFERENCES

1. WJ. Stadelman, Eggs and egg products. Encyclopedia of Food Science and Technology; Wiley and sons, Newyork (2000).
2. NY. Mezenner, A. Bensmaili, Chem. Engin. J., 147, 87–96 (2009).
3. Z. Wei, C. Xu, B. Li, Bioresour Technol., 100, 2883–5 (2009).
4. S. Yoo JS. Hsieh, P. Zou, J. Kokoszka, Bioresource Technology., 100, 6416–21 (2009).
5. WH. Eisa, YK. Abdel-Moneam, Y. Shaaban, AA. Abdel-Fattah, AMA. Zeid, Mater Chem Phys., 128, 109–13 (2011).
6. T-X. Fan, S-K Chow, D. Zhang, Prog Mater Sci., 54, 542–659 (2009).
7. W. Zhang, D. Zhang, T. Fan J. Gu, J. Ding, H. Wang, et al, Chem Mater., 21, 33–40 (2008).
8. AA. Ghani, R. Santiagoo, AC. Johnson, N. Ibrahim, S. Selamat., IcoSM (2007).
9. PS. Ratna, PS. Padhi, Pollution Due to Synthetic Dyes Toxicity & Carcinogenicity Studies and Remediation. Int. Env. Science., 3, 940 – 955 (2012).
10. S. Srivastava, R. Sinha, D. Roya, Aquatic Toxicology., 66, 319–329 (2004).
11. Food standards Australia newzeland, Malachite green in aquacultured fish. http://www.foodstandards.gov.au/consumer/chemicals/malachitegreen/Pages/default.aspx
12. R. Mirzajani, S. Ahmadi, Indust. Engin. Chem., 23, 171-178 (2015).
13. S. Namrodi, M. Golipor, H. Mirrezai, M. Mazandarani, National conference about planning of environmental protection (2013).
14. G. Alsenani, J. Amer. Scien., 9, 30-35 (2013).
15. LK. Akinola, AM. Umar, J. Appl. Sci. Environ. Manage., 19, 279 – 288 (2015).
16. F. Moeinpour, A. Alimoradi, M. Kazemi, J. Envir. Health. Sci. Eng., 12, 112 (2014).
17. ND. Pragnesh, K. Satinder, K. Ecta, J. Chem.ech., 18, 53-60 (2011).
18. NN. Nasssar, NM. Marei, G. Vitale, LA. Arar, Chem. Engin. 93 (2015).
19. Kanchi. Suvardhan, Environ. Anal. Chem (2014).
20. G. Sreelatha, V. Ageetha, J. Parmer, P. Padmaja, J. Chem. Engin. Data., 56, 35-42 (2010).
21. M. Torab-Mostaedi, M. Asadollahzadeh, A. Hemmati , A. Khosravi, J. Taiwan Inst. Chem. Eng., 44, 295-302 (2013).
22. NM. Mahmoodi, B. Hayati, M. arami, C. Lan, Adsorption of textile dyes on Pine cone from colored wastewater: Kinetic, equilibrium and thermodynamic studies. Desalination., 268, 117-125 (2010).
23. F. Deniz, S. Karaman, Chem. Eng. J., 170, 67-74 (2011).
24 CA. Almeide, NA. Debacher, AJ. Downs, L. Cottet, CA. Mello, J. Colloid interface SCI., 332, 46-53 (2009).
25. C. Namasivayam, N. Kanchana, Chemosphere., 25, 1691–1706 (1992).
26. S. Kaur, S. Rani, RK. Mahajan, J. Chem (2011).
27. O. Serpil, K. Fikret, Environ. Manage., 81, 307–314 (2006).
28. Y. Bulut, N. Gozubenli, H. Aydin, Hazard. Mater., 144, 300–306 (2007).
29. G. Sreelatha, V. Ageetha, J. Parmar, P. Padmaja, G. Chem. Eng., 56, 35-42 (2014).
30. R. Lafi, AB. Fradj, A. Haiane, BH. Hameed, Korean. J. Chem. Eng., 1-9 (2014).
31. F. Ovaisi, M. Nikazar, MH. Razagi, National conference about planning of environmental protection (2012).
32. W. WU, Q. He, C. Jiang, Nanoscale Res Lett., 33, 97–415 (2008).
33. F. Bandari, F. Safa, SH. Shariati, Science. Engin., 40, 3363-3372 (2015).
34. M. Golshekan, SH. Shariati, Acta. Chim. Slov., 60, 358-367 (2013).
35. M. Manoochehri, SM. Mostashari, Shariatim S.H, Cell. Chem. Tech., 47, 727-734 (2013).
36. SH. Shariati, M. Faraji, Y. Yamini, AA. Rajabi, Else. Desal., 270, 160-165 (2011).
37. N. Yang, S. Zhu, D. Zhang, S. Xu, Mater. Lett., 62, 645–647 (2008).

38. J. Park, K. An, Y. Hwang, JG. Park, HJ. Noh, JY. Kim, JH. Park, NM. Hwang, T. Hyeon, Nat. Mater., 3, 891–895 (2004).
39. JH. Jang, HB. Lim, Microchem., 94, 148–158 (2010).
40. S. Ahmadi, A. Rahdar, S. Rahdar, C.A. Igwegbe, Desalination and water treatment, 152, 401-410 (2019).
41. A. Rahdara, S. Ahmadi, J. Fu, S. Rahdar, Desalination and water treatment., 137, 174-182 (2019).
42. S. Rahdar, A. Rahdar, C.A. Igwegbe, F. Moghaddam, S. Ahmadi, Desalination and water treatment., 141, 386-393 (2019).
43. A. M.Khan, F. Shafiq, S. A. Khan, S. Ali, B. Ismail, A. S. Hakeem, A. Rahdar, M. F. Nazar, M. Sayed, A. R. Khana, J. molecular liquids., 274, 673-680 (2019).
44. I. Langmuir, The adsorption of gases on plane surfaces of glass, mica and platinum. Am. Chem. Soc., 40, 1361–1403 (1918).
45. HMF. Freundlich, Over the adsorption in solution. Z. Phys. Chem., 57, 385–470 (1906).
46. MJ. Tempkin, V. Pyzhev, Recent modifications to langmuir isotherms. Acta Physiol. Chem. USSR., 12, 271(1940).